Catalyst Regeneration Kinetics in the Presence of Pore Blockage

A model is developed for fluid-solid reaction kinetics in a porous solid. The model is based on a convergent-divergent pore structure and accounts for pore blockage and inside cavities. A numerical study applied the model to the process of coke removal for catalyst regeneration. The calculated results show that in the presence of pore occlusion, the reaction rates are significantly reduced at the beginning of reaction. At higher levels of coke loading the reaction behavior can be especially affected by the volume fraction of the divergent pores. This behavior can be used to select catalysts with pore structures that improve control of the regeneration process.

Yuli Chang and D. D. Perlmutter
Department of Chemical Engineering
University of Pennsylvania
Philadelphia, PA 19104

Introduction

Among the many heterogeneous reactions between a solid and a fluid that are industrially significant, an important subgroup involves partial oxidation of a carbonaceous surface. Because of this feature in common, it might be expected that reactions such as char gasification, production of activated carbon, and regeneration of coked catalyst would be described by related models. In fact, striking similarities have been observed between the former two reactions, particularly that the reaction rates show maxima at intermediate conversion levels (Kawahat and Walker, 1962; Jenkins et al., 1973; Hippo and Walker, 1975; Tomita et al., 1977; Dutta et al., 1977; Dutta and Wen, 1977; Hashimoto et al., 1979; Chin et al., 1983; Su and Perlmutter, 1985). Catalyst regeneration kinetics can show various patterns of reaction behavior, including also one that exhibits a maximum in rate with respect to conversion (Haldeman and Botty, 1959; Weisz and Goodwin, 1966).

For char gasification and carbon activation, the studies referenced above have demonstrated that the physical structure of the solid reactant changes continuously as reaction proceeds, and this evolution of pore structure affects the reaction kinetics by altering the available surface area. The structural changes that accompany the char gasification reaction have been described by a random pore model by Bhatia and Perlmutter (1980), and independently by Gavalas (1980). Further details of the evolving pore size distribution have been added by Su and Perlmutter (1985).

Even though successful application of the random pore model has been demonstrated for char gasification, interpretation of catalyst regeneration kinetics via this model is complicated by the heterogeneity of the solid phase involved in this reaction system. The major difference between reactions such as char gasification and carbon activation on the one hand, and regeneration of coked catalyst on the other, is that the surface on which the former two reactions occur is the entire surface of the solid, whereas that for the latter does not include the noncoked surface of the underlying catalyst.

The reaction kinetics in the presence of such an inert support phase was discussed by Chang and Perlmutter (1987); however, no consideration was given to possible occlusion of pore space by coke deposition. The work presented here is a sequel to the earlier investigation with the specific aim of accounting for the reaction kinetics in the presence of pore occlusion. For this purpose, a computational model is developed that considers a bundle of nonintersecting convergent-divergent pores to represent the pore structure of the inert support. This model allows for possible pore mouth blockage as well as inside cavities, and follows that proposed by Foster and Butt (1966). It differs from the earlier work in that the volume fraction of the centrally divergent pores need not be equal to that of the centrally convergent pores. Instead, the overall pore length of the inert support is divided into two parts for divergent and convergent pores, according to the respective volume fractions. The total number of pores is also included as a parameter.

Model Development

The model proposed by Chang and Perlmutter (1987) interpreted catalyst regeneration kinetics in terms of the interaction between the catalyst (inert support) pore structure and the coke (reacting material) distribution in the pores. It was assumed that all the internal surface of the catalyst was initially covered by deposited coke and that the regenerative oxidation took place

on the inner surface of the coke earlier deposited in the pores. In the absence of occlusion of pore space by the coke each pore of the catalyst particle has associated with it a growing surface as the reaction progresses. As the pores enlarge and the various reaction surfaces in the particle grow, islands of nonreacting surface of the catalyst will emerge as the coke covering them is consumed. Wherever bare catalyst surface emerges, a pore will cease its growth, and collectively the development of the overall surface area of the particle will slow down.

Pore volume distribution of catalyst

Consider the surface of the catalyst to arise from a bundle of nonintersecting pores, each with a circular cross section but not necessarily a cylinder, and consider the pore sizes to be described by a measurable pore volume distribution function $f(r)$. Then the total pore volume is

$$V = \int_{r_N}^{r_W} f(r)\, dr \tag{1}$$

the total pore surface is

$$S = 2\int_{r_N}^{r_W} \frac{f(r)}{r}\, dr \tag{2}$$

and the cumulative pore length is

$$L = \frac{1}{\pi}\int_{r_N}^{r_W} \frac{f(r)}{r^2}\, dr \tag{3}$$

where the range of pore sizes is between a smallest radius r_N and a largest r_W.

Pore shapes

To account for the reaction kinetics in the presence of pore occlusion by coke deposition, the set of nonintersecting pores in the catalyst is considered to consist of two different types of pores, one of volume fraction α and widest at the center (divergent), the other of fraction $(1 - \alpha)$ and narrowest at the center (convergent). Each of these sets has N pores. Schematic representation of the divergent and the convergent pores is shown in Figure 1, in which the hypothesized pores are divided into two halves, each a mirror image of the other. The conical halves of the divergent and convergent pores are geometrically identical, i.e., the radial pore size at a given relative position on the height of the halfpore is the same.

Pore volume distribution of coke

Consider the volume of coke deposited on the inner surfaces of the divergent pores to be described by a volume distribution function $g_d(r)$. Thus, the total volume of coke deposited in the divergent pores is:

$$V_{Rd} = \int_{r_N}^{r_W} g_d(r)\, dr \tag{4}$$

Using the expression for the volume of an annulus

$$g_d(r)\, dr = \pi\alpha[r^2 - [r - h_{d0}(r)]^2]\, dL, \quad r_N < r \le r_W \tag{5}$$

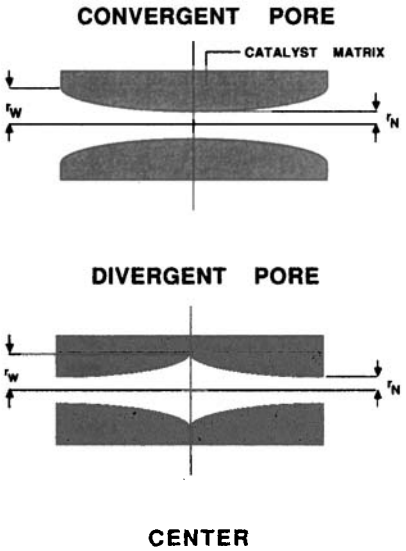

Figure 1. Schematic representation of convergent and divergent pores.

where the differential pore length is

$$dL = \frac{f(r)}{\pi r^2}\, dr \tag{6}$$

and $h_{d0}(r)$ is the initial coke annular layer thickness in the divergent pores. Since for a divergent pore the thickness of this layer in the blocked regime is the radius of the pore mouth, combining Eqs. 5 and 6 gives

$$h_{d0}(r) = \begin{cases} r_N, & r = r_N \\ \left[1 - \sqrt{1 - \dfrac{g_d(r)}{\alpha f(r)}}\right] r, & r > r_N \end{cases} \tag{7}$$

In parallel to the foregoing consider the volume of coke deposited in the convergent pores to be described by a volume distribution function $g_c(r)$. The sizes of the unblocked portions in the convergent pores exist over the range between r_b and r_w, where r_b denotes the largest pore size of coke blockage, as shown in Figure 2a. The total volume of coke deposited in the unblocked portions of the convergent pores is

$$V_{Rc} = \int_{r_b}^{r_W} g_c(r)\, dr \tag{8}$$

Using once again the expression for the volume of an annulus

$$g_c(r)\, dr = \pi(1 - \alpha)[r^2 - [r - h_{c0}(r)]^2]\, dL, \quad r > r_b \tag{9}$$

where $h_{c0}(r)$ is the initial coke annular layer thickness for this case. Since the thickness of the coke annular layer in the blocked portion is equal to r, combining Eq. 9 with Eq. 6 and rearranging gives

$$h_{c0}(r) = \begin{cases} r, & r \le r_b \\ \left[1 - \sqrt{1 - \dfrac{g_c(r)}{(1 - \alpha) f(r)}}\right] r, & r > r_b \end{cases} \tag{10}$$

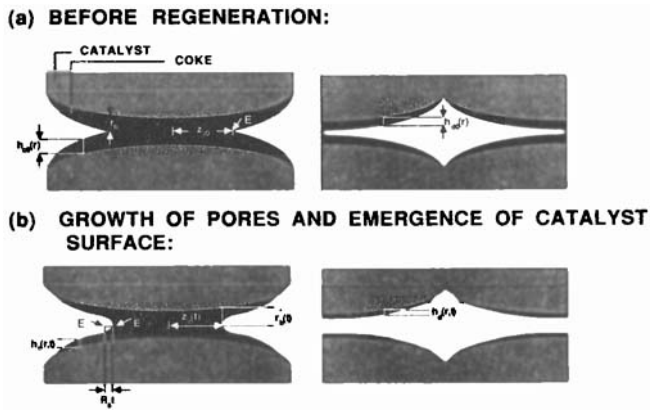

Figure 2. Schematic representation of coke deposition in convergent and divergent pores.

Blockage of pores

The growth of the total reaction surface in a coked catalyst containing pore blockages and inside cavities may be followed in terms of the growth of the unblocked portions and that of the blocked portions, as shown in Figure 2b. If under kinetic-controlled conditions the rate of reaction is proportional to the total surface area

$$\frac{d[h_d(r,t)]}{dt} = -R_s, \quad r > r_N \tag{11}$$

$$\frac{d[h_c(r,t)]}{dt} = -R_s, \quad r > r_b \tag{12}$$

and

$$\frac{d[z_c(t)]}{dt} = -R_s \tag{13}$$

where $h_d(r,t)$ and $h_c(r,t)$ denote respectively the coke annular layer thicknesses in the unblocked portions of the pores at any time; and $z_c(t)$ is the half length of coke blockage in the convergent pores at any time.

The initial length of the coke blockage in the convergent pores can be expressed as:

$$z_{c0} = \frac{(1-\alpha)}{2\pi N}\int_{r_N}^{r_b}\frac{f(\xi)}{\xi^2}\,d\xi \tag{14}$$

and the total volume of coke in the blockage is:

$$V_{Rb} = (1-\alpha)\int_{r_N}^{r_b} f(\xi)\,d\xi \tag{15}$$

Consider the growth of the unblocked portions of the set of pores to be in the radial direction only. Following the treatment adopted by Chang and Perlmutter (1987), one can obtain the total volume of coke deposited in the divergent pores at any time as

$$V^*_{Rd}(t) = \alpha\int_{r_N}^{r_w}[r^2 - [r - h_d(r,t)]^2]\frac{f(r)}{r^2}\,dr \tag{16}$$

The total volume of coke in the unblocked portions of the convergent pores at any time is:

$$V^*_{Rc}(t) = (1-\alpha)\int_{r_b}^{r_w}[r^2 - [r - h_c(r,t)]^2\frac{f(r)}{r^2}\,dr \tag{17}$$

If in addition to the radial change, one considers the removal of coke in the axial direction, the process starts at point E of the coke plug (Figure 2a). When the length of the coke blockage z_{c0} is much larger than the largest radial pore size of the coke plug r_b, the total volume of coke removed from the blockage at any time may be approximated by the equation

$$V^*_{Rp}(t) = \begin{cases} \dfrac{4}{3}\pi N(R_s t)^3, & t \le t_p \\ (1-\alpha)\left[\displaystyle\int_{r_b^*}^{r_b} f(\xi)\,d\xi\right], & t > t_p \end{cases} \tag{18}$$

where $r_b^*(t)$ denotes the pore size of the cross-section that is tangent to the surface at point E' (Figure 2b), implicitly defined by

$$\int_{r_N}^{r_b^*}\frac{f(\xi)}{\xi^2}\,d\xi = \begin{cases} \dfrac{2N\pi}{(1-\alpha)}z_c(t), & t \le t_c \\ 0, & t > t_c \end{cases} \tag{19}$$

and t_p and t_c denote the time periods required: 1) for the distance between E and E' to evolve to r_b; and 2) for the coke blockage in the convergent pores to be consumed. Then the total volume of coke involved in the blockage of the convergent pores at any time is:

$$V^*_{Rb}(t) = V_{Rb} - V^*_{Rp}(t) \tag{20}$$

Adding Eqs. 16, 17 and 20 to account for the several contributions, the overall volume of coke in the composite at any time is

$$V^*_R(t) = \alpha\int_{r_N}^{r_w}[r^2 - [r - h_d(r,t)]^2]\frac{f(r)}{r^2}\,dr + (1-\alpha)\left[\int_{r_b}^{r_w}[r^2 - [r - h_c(r,t)]^2]\frac{f(r)}{r^2}\,dr + \int_{r_N}^{r_b} f(\xi)\,d\xi\right] - V^*_{Rp}(t) \tag{21}$$

From the definition of conversion:

$$X = 1 - \frac{V^*_R(t)}{V_R} \tag{22}$$

and the conversion-time relationship for this fluid-solid reaction is the simple combination of Eqs. 21 and 22.

Reaction rate

Because of the pore mouth blockages, the reacting surfaces in the inner portions of the divergent pores are not accessible to the fluid reactant at the beginning of reaction. As a result the reac-

tion rate cannot be obtained directly by differentiating the conversion function and must be derived independently.

The total reacting surface area in the unblocked portions of the divergent pores is:

$$S^*_{Rd}(t) = \begin{cases} 0, & t = 0 \\ 2\alpha \int_{r_N}^{r_W} H_d(r,t)[r - h_d(r,t)] \dfrac{f(r)}{r^2}\, dr, & t > 0 \end{cases} \tag{23}$$

where $H_d(t)$ is the Heaviside step function:

$$H_d(r,t) = \begin{cases} 1, & t < \dfrac{h_{d0}(r)}{R_s} \\ 0, & t \geq \dfrac{h_{d0}(r)}{R_s} \end{cases} \tag{24}$$

introduced here because reaction stops when the covering coke is removed and the catalyst surface is exposed. For the unblocked portions of the convergent pores, the reacting surface area at any time is:

$$S^*_{Rc}(t) = 2(1-\alpha) \int_{r_b}^{r_W} H_c(r,t)[r - h_c(r,t)] \frac{f(r)}{r^2}\, dr \tag{25}$$

where

$$H_c(r,t) = \begin{cases} 1, & t < \dfrac{h_{c0}(r)}{R_s} \\ 0, & t \geq \dfrac{h_{c0}(r)}{R_s} \end{cases} \tag{26}$$

The reacting surface of coke blockage in the divergent pores is:

$$S^*_{bd}(t) = \begin{cases} 2\pi N r_N^2, & t = 0 \\ 0, & t > 0 \end{cases} \tag{27}$$

Assuming an isotropic process of removal of coke from the blockage, the reacting surface area in the blocked portion of the convergent pores may be approximated as:

$$S^*_{bc}(t) = \begin{cases} 4\pi N (R_s t)^2, & t \leq t_p \\ 2\pi N [r^*_b(t)]^2, & t > t_p \end{cases} \tag{28}$$

Adding Eqs. 23, 25, 27 and 28, one obtains the overall reacting surface area in the coked catalyst at any time:

$$S^*_R(t) = \begin{cases} 2\pi N r_N^2 + S^*_{Rc}(t) + S^*_{bc}(t), & t = 0 \\ 2\alpha \displaystyle\int_{r_N}^{r_W} H_d(t)[r - h_d(r,t)] \frac{f(r)}{r^2}\, dr & \\ \quad + S^*_{Rc}(t) + S^*_{bc}(t), & t > 0 \end{cases} \tag{29}$$

If the rate of reaction is proportional to the total surface area:

$$\frac{dX}{dt} = \frac{R_s}{V_R} S^*_R(t) \tag{30}$$

and the rate-time relationship of the fluid-solid reaction is the combination of Eqs. 29 and 30, which may in turn be combined with Eq. 25 to express the result in terms of the coke volume distribution functions $g_d(r)$ and $g_c(r)$.

Coke loading

In a prior report (Chang and Perlmutter, 1987) it was shown that for a coke distribution that is proportional to the pore length distribution, the process of deposition ceases when the divergent pores seal at a critical coke loading. As a result, for any level of coke loading above the critical the volume of coke in these pores remains constant at

$$V_{Rd} = \alpha V_{\text{cri}} \tag{31}$$

where V_{cri} denotes the critical volume. It was shown in the same reference that the coke volume distribution at levels above the critical is

$$g_d(r) = \frac{\alpha V_{\text{cri}} f(r)}{\pi r^2 L}, \quad r_N < r \leq r_W \tag{32}$$

The corresponding distribution in the unblocked portions of the convergent pores can be written as

$$g_c(r) = \frac{V_{Rc} f(r)}{r^2 \left[\pi L - \displaystyle\int_{r_N}^{r_b} \frac{f(\xi)}{\xi^2}\, d\xi\right]}, \quad r_b < r \leq r_W \tag{33}$$

Substituting Eq. 32 into Eq. 7, one obtains an expression for the thickness of coke annular layer in the divergent pores. Similarly, substituting Eq. 33 into Eq. 10 gives the expression for the thickness of coke layer in the convergent pores.

Number of pores

By assuming radial burnoff of reacting material within the unblocked portions of pores, it has implicitly been assumed that within those portions the circumferential surface area of the coke annulus at the pore entrance is negligible in comparison with the conical surface area within the pore; that is, as shown in Figure 3:

$$S_1 \ll S_2 \tag{34}$$

To meet this criterion requires that the initial length of the unblocked portion of the pore be much larger than the thickness of the coke annular layer at the pore entrance. For a divergent pore, the length of the unblocked portion before reaction is

$$z^*_{d0} = \frac{\alpha L}{2N} \tag{35}$$

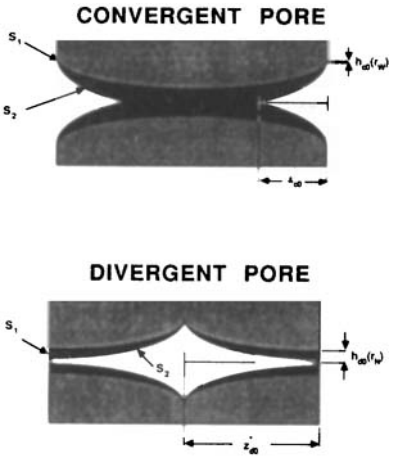

Figure 3. Circumferential coke surface area S_1 and conical surface area S_2.

Since

$$z_{a0}^{*} \gg r_N \tag{36}$$

an upper bound on the number of pores is

$$N \ll \frac{\alpha L}{2r_N} \tag{37}$$

A similar inequality can be developed for a convergent pore, but the result is not useful, since it is always less restrictive than inequality (Eq. 37).

Numerical Evaluations

In assessing the implications of the model presented here a series of numerical simulations were carried out, focusing especially on the effects of pore blockage on coke layer thickness and regeneration rate. To this end it was necessary to estimate the essential parameters in the model:

- The pore volume distribution function $f(r)$
- The volume fraction of the divergent pores α
- The radial pore sizes r_N and r_W of the catalyst, and r_b for the coke blockage in the convergent pores
- The overall coke volume V_R

The pore sizes and volume distribution given for an uncoked catalyst by Haldeman and Botty (1959) were used for $f(r)$ as well as to obtain $r_N = 1.2 \times 10^{-9}$ m and $r_W = 1.5 \times 10^{-8}$ m. The same source provided $V = 4.2 \times 10^{-4}$ m^3/kg. Values of several other parameters could be chosen over reasonable ranges but not entirely arbitrarily, since they had to be consistent with the prior data. Within these limitations the choices made for particular effects being studied were:

$$2.1 \times 10^{-5} \le V_R \le 1.26 \times 10^{-4}\ \text{m}^3/\text{kg}$$

$$1.32 \times 10^{-9} \le r_b \le 2.76 \times 10^{-9}\ \text{m}$$

$$0.1 \le \alpha \le 0.3$$

The range of values of α were suggested by the data of Drake (1949).

Upper bounds on the number of pores were obtained from inequality (Eq. 37) to give:

α	Upper Bound on N
0.1	3.24×10^{17}
0.2	6.47×10^{17}
0.3	9.71×10^{17}

and numerical estimates were made by assuming actual values of N to be less than the upper bounds by two orders of magnitude. The appropriate parameter values were inserted into Eq. 30 to compute rates of reaction and into Eqs. 7 and 10 to find the corresponding coke profiles.

Results and Discussion

Pore blockage and inside cavities

The effect on reaction kinetics of the existence of pore mouth blockages and inside cavities is demonstrated in Figure 4 by superimposing the results of this study on those computed earlier by Chang and Perlmutter (1987) from the experimental data of Haldeman and Botty for the case where no blockage existed. From this comparison the pattern of reaction behavior in the presence of occlusion of pore space is in general similar to that in the absence of occlusion, but the computed rates of reaction in the former case are significantly reduced at the start of regeneration, because the blockage at the pore entrance makes the coke deposited in the divergent pores initially inaccessible to oxygen.

The coke profiles in both the divergent and convergent pores are presented in Figure 5, showing two different but very similar results. For divergent pores the profile begins at point A (1, 1) on this normalized scale, since the entrances to the divergent pores are blocked. For convergent pores, the initial portion of the profile AB shows increasing thickness of coke between radii 1.0 and 1.1, the range where the pores are blocked and $h_{c0}(r) = r$.

For a given pore size the coke annular layer in the convergent pores is thicker than that in the divergent pores, because the pro-

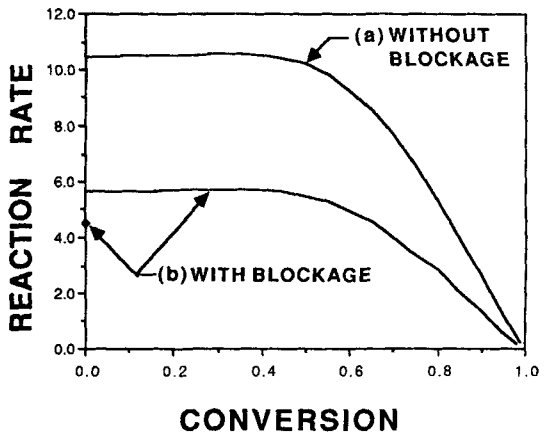

Figure 4. Comparison of reaction rates in the absence of pore occlusion with those in its presence.

Data are normalized with respect to rates at conversion = 0.075 and conversion is based on fractional coke removal. Curve a is for the normalized coke volume $\bar{V} = 0.05$; curve b is for $\bar{V} = 0.09$, $\alpha = 0.2$, and the normalized largest blockage size $\bar{r}_b = 1.1$. The coke volume and the largest blockage size are normalized with respect to $V = 4.2 \times 10^{-4}$ m^3/kg and $r_N = 1.2 \times 10^{-9}$ m, respectively.

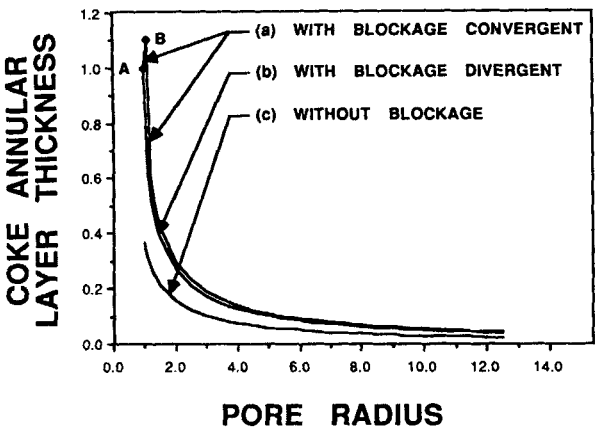

Figure 5. Comparison of coke profiles in the absence of pore occlusion with those in its presence.

Thickness and pore radius are normalized with respect to $r_N = 1.2 \times 10^{-9}$ m. Curves a and b are for $\bar{V} = 0.09$, $\alpha = 0.09$, and $\bar{r}_b = 1.1$.

cess of coke deposition in the convergent pores does not stop at the critical V_{cri}. The coke layer is reduced in thickness in the absence of occlusion of pore space, because the coke loading used in the computation is less than the critical. As a consequence the reaction surface area of the catalyst is larger. This is consistent with the higher rates of reaction already seen in Figure 4.

Coke deposition pattern

The effect on coke thickness of the geometry of the deposit is demonstrated in Figure 6, in which the profiles presented are for different values of r_b with the same level of coke loading. The normalized profiles for the divergent pores fall on the same curve, because as noted above the process of coke deposition in the divergent pores stopes as soon as the entrance is blocked.

Two opposing factors are involved in determining the thickness of the coke layer in the unblocked portions of the convergent pores: first, a larger fraction of the coke is deposited in the blocked portions for either larger r_b or smaller α, tending to give a thinner coke layer; and second, the total pore length of the

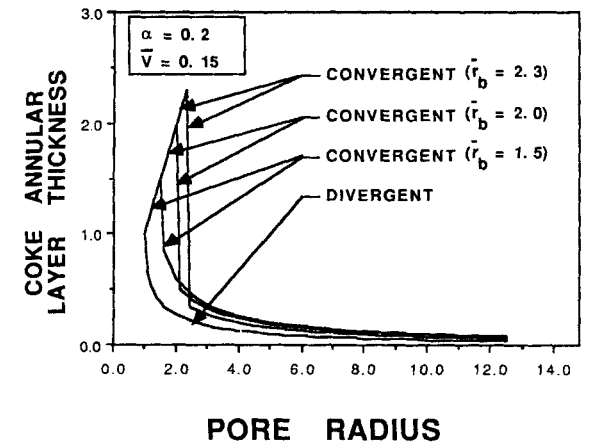

Figure 6. Coke profiles for different coke deposition patterns.

Thickness and pore radius are normalized with respect to $r_N = 1.2 \times 10^{-9}$ m.

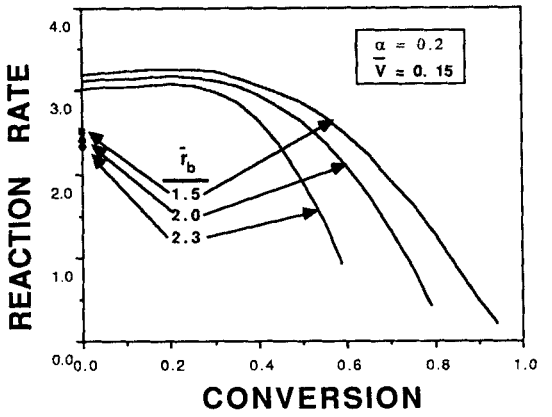

Figure 7. Reaction rates at different conversions for several coke deposition patterns.

unblocked portions in the convergent pores is smaller for either larger r_b or larger α, thus fostering a thicker layer. That the first of these factors is dominant in the convergent pores is shown by the profiles in Figure 6.

A reverse trend is found in the observations of Figure 7, in which increased reaction rates are found for smaller values of r_b, showing that in the presence of coke blockage the thickness is not the only factor that affects the area of the reaction surface in the convergent pores. A larger fraction of unblocked portion in the convergent pores is associated with a smaller value of r_b to give a larger reaction surface area. Figure 7 shows that the effect of the fraction of unblocked portions in the convergent pores overcomes that of the thickness of coke layer in determining the reaction surface area. The process of emergence of islands of nonreactive surface is favored by the pattern of deposition associated with large r_b. A related trend may be found in Figure 7, where a shallow maximum in rate occurs for small conversions and large values of r_b.

For larger values of r_b not only is a larger amount of coke deposited in the blockage than in the unblocked portion of a pore, but in addition the coke deposited in the blockage has a much smaller reaction surface area. As a result the rate falls close to zero at a lower conversion level, as presented in Figure 7. With reduced rates as r_b increases, the time period required for complete conversion is longer.

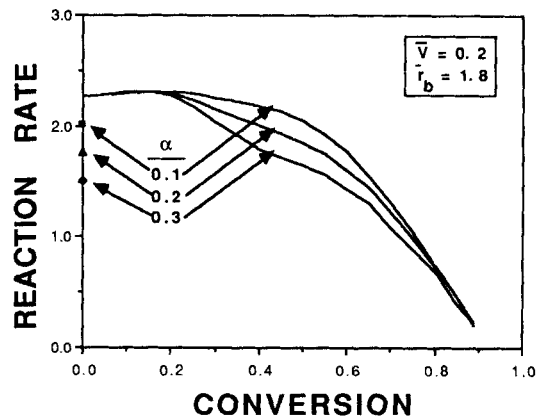

Figure 8. Reaction rates for pore structures with different levels of α for $\bar{V} = 0.2$ and $\bar{r}_b = 1.8$.

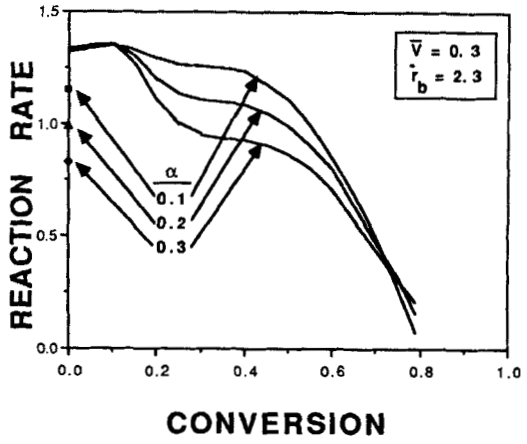

Figure 9. Reaction rates for pore structures with different levels of α for $\bar{V} = 0.3$ and $\bar{r}_b = 2.3$.

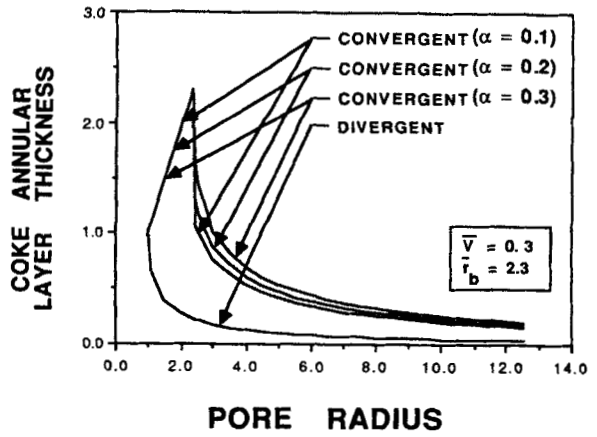

Figure 11. Coke profiles for different pore structures with $\bar{V} = 0.3$ and $\bar{r}_b = 2.3$.

Effect of pore structure

Figures 8 and 9 demonstrate that the catalyst pore structure has a significant impact on the way in which reaction rates change with conversion. As the volume fraction of the divergent pores increases, for example, an inflection point develops at an intermediate conversion level. This change in the shape of the pattern of reaction behavior appears in Figure 8 but not in Figure 9, suggesting that the level of coke loading also has a significant impact on the pattern of reaction behavior.

The corresponding coke profiles are presented in Figures 10 and 11, in which one can note that the difference among coke profiles in the unblocked portions of the convergent pores becomes notable with an increase in loading. At any level of coke loading the same two opposing factors are involved in determining the thickness of the coke layer in the unblocked portions of the convergent pores as was noted above: first, less coke is deposited in the unblocked portions of the convergent pores for larger α, and second, the total pore length of unblocked portions of the convergent pores is smaller for larger α. The former factors tends to give a thinner coke layer, while the latter tends to give a thicker one. It is shown in Figures 10 and 11 that the coke layer is in fact thicker for larger α, indicating that of these two the smaller total pore length is the dominant factor.

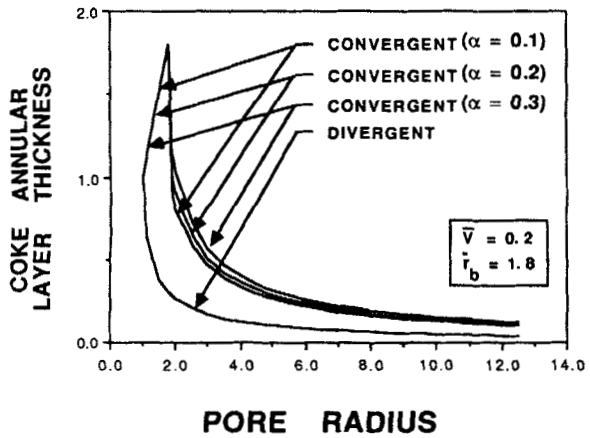

Figure 10. Coke profiles for different pore structures with $\bar{V} = 0.2$ and $\bar{r}_b = 1.8$.

Coke loading

Distinctions between the effects of convergent and divergent pores depend on the level of coke loading. At a loading level of $V_R = 4.2 \times 10^{-5}$ m^3/kg, for example, profiles in the unblocked portions of convergent pores are almost the same as those in divergent pores for all the structures studied. As a consequence the surface areas and reaction rates are the same. For higher levels of coke loading, on the other hand, layers in the unblocked parts of the convergent pores are much thicker than those in the divergent pores (see Figure 10 for $V_R = 8.4 \times 10^{-5}$ m^3/kg), and as a result the emergence of islands of unreactive surface in the divergent pores affects the overall surface area of the pore structure and hence the reaction kinetics. This point is illustrated in Figure 8, where the reaction rates are reduced in the intermediate stages of regeneration for increases in α.

For $V_R \geq 8.4 \times 10^{-5}$ m^3/kg the emergence of nonreactive surface occurs first in the divergent pores, and the development of the rate of reaction exhibits a slight shallow maximum in the initial stages of regeneration (shown in Figures 8 and 9). As the reaction continues, the loss of reaction surface associated with the depletion of coke in the divergent pores is compensated for by the opposing effect of the growth of reaction surface associated with the convergent pores. This is illustrated by a slight knee in the rate curves over some intermediate conversion levels. Ultimately the rate of reaction diminishes with conversion as the loss of reaction surface prevails.

Acknowledgment

This research was funded partly by the U.S. Department of Energy under contract No. DE-AC21-81MC-161.

Notation

$f(r)$ = pore volume distribution of porous catalyst
$g_d(r)$ = volume distribution of coke in divergent pores
$g_c(r)$ = volume distribution of coke in convergent pores
$h_{d0}(r)$ = thickness of annular layer of coke at $t = 0$ in divergent pores
$h_{c0}(r)$ = thickness of annular layer of coke at $t = 0$ in convergent pores
$h_d(r, t)$ = thickness of annular layer of coke at any time in divergent pores
$h_c(r, t)$ = thickness of annular layer coke at any time in convergent pores
$H_c(t)$ = Heaviside step function defined in Eq. 26
$H_d(t)$ = Heaviside step function defined in Eq. 24

L = overall pore length of porous media
N = number of pores
r = radial pore size
$\bar{r}$ = dimensionless radial pore size
r_b = largest radial pore size of coke blockage in convergent pores
$\bar{r}_b = r_b/r_N$
$r_b^*(t)$ = largest radial pore size of coke blockage in convergent pores at any time
r_N = smallest radial pore size of porous media
r_W = largest radial pore size of porous media
R_s = kinetic-controlled surface reaction rate
S = overall pore surface area of porous media
S_1 = circumferential surface area of coke annulus at pore entrance
S_2 = conical surface area of coke annulus in the unblocked portion of a halfpore
$S_R^*(t)$ = overall surface area at any time
$S_{Rc}^*(t)$ = total reacting surface area in the unblocked portions of convergent pores at any time
$S_{Rd}^*(t)$ = total reacting surface area in the unblocked portions of divergent pores at any time
$S_{bc}^*(t)$ = total reacting surface area in the blocked portions of convergent pores at any time
$S_{bd}^*(t)$ = total reacting surface area in the blocked portions of divergent pores at any time
t = time
t_c = time period for removal of coke from the blocked portion of a convergent halfpore
$t_p = (r_b/R_s)$ = the time period required for $r_b^*(t)$ to evolve to r_b
V = overall price volume of porous media
$\bar{V}$ = volume ratio of V_R to V
V_{cri} = critical coke volume for pore occlusion
V_R = overall volume of coke
$V_R^*(t)$ = overall volume of coke at any time
V_{Rb} = total volumm of coke in the blocked portions of convergent pores at $t = 0$
$V_{Rb}^*(t)$ = total volume of coke in the blocked portions of convergent pore as at any time
V_{Rc} = total volume of coke in the unblocked portions of convergent pore at $t = 0$
V_{Rc}^* = total volume of coke in the unblocked portions of convergent pores at any time
V_{Rd} = total volume of coke divergent pores at $t = 0$
$V_{Rd}^*(t)$ = total volume of coke in the unblocked portions of divergent pores at any time
$V_{Rp}^*(t)$ = total volume of coke removed from the blocked portions of convergent pores at any time
X = conversion
z_{c0} = length of coke blockage in a convergent halfpore at $t = 0$
$z_c(t)$ = length of coke blockage in a convergent halfpore at any time
z_{d0}^* = length of unblocked portion in a divergent halfpore at $t = 0$

Greek letters

α = volume fraction of divergent pores
ξ = dummy variable

Literature Cited

Bhatia, S. K., and D. D. Perlmutter, "A Random Pore Model for Fluid-Solid Reactions: I. Isothermal, Kinetic Control," *AIChE J.*, **26**, 379 (1980).

Chang, Y., and D. D. Perlmutter, "Effect of Pore-Distributed Coke on Catalyst Regeneration Kinetics," *AIChE J.*, **33**, 940 (June, 1987).

Chin, G. S., S. Kimura, S. Tone, and T. Otake, "Gasification of Coal Char with Steam: I. Analysis of Reaction Rate," *Int. Chem. Eng.*, **23**, 105 (1983).

Drake, L. C., "Pore-Size Distribution in Porous Materials," *Ind. Eng. Chem.*, **41**, 780 (1949).

Dutta, S., C. Y. Wen, and R. J. Belt, "Reactivity of Coal and Char: I. In Carbon Dioxide Atmospheres," *Ind. Eng. Chem. Proc. Des. Dev.*, **16**(1), 20 (1977).

Dutta, S., and C. Y. Wen, "Reactivity of Coal and Char: II. In Oxygen-Nitrogen Atmospheres," *Ind. Eng. Chem. Proc. Dev.*, **16**(1), 31 (1977).

Foster, R. N., and J. B. Butt, "A Computational Model for the Strucutre of Porous Materials Employed in Catalysis," *AIChE J.*, **12**, 180 (Mar., 1966).

Gavalas, G. R., "A Random Capillary Model with Application to Char Gasification at Chemically Controlled Rates," *AIChE J.*, **26**, 577 (Mar., 1980).

Haldeman, R. G., and M. C. Botty, "On the Nature of the Carbon Deposit of Cracking Catalysis," *J. Phys. Chem.*, **63**, 489 (1959).

Hashimoto, K., K. Miura, F. Yoshikawa, and I. Imai, "Change in Pore Structure of Carbonaceous Materials During Activation and Adsorption Performance of Activated Carbon," *Ind. Eng. Chem. Proc. Dev.*, **18**, 73 (1979).

Hippo, E., and P. L. Walker, Jr., "Reactivity of Heat-Treated Coals in Carbon Dioxide at 900 C," *Fuel*, **54**, 245 (1975).

Jenkins, R. G., S. P. Nandi, and P. L. Walker, Jr., "Reactivity of Heat-Treated Coals in Air at 500 C," *Fuel*, **52**, 288 (1973).

Kawahata, M., and P. L. Walker, "Mode of Porosity Development in Activated Anthracite," *Proc. Carbon Conf.*, **2**, 251, Pergamon Press (1962).

Su, J.-L., and D. D. Perlmutter, "Effect of Pore Structure on Char Oxidation Kinetics," *AIChE J.*, **31**, 973 (June, 1985).

Tomita, A., O. P. Mahajan, and P. L. Walker, Jr., "Reactivity of Heat-Treated Coals in Hydrogen," *Fuel*, **56**, 137 (1977).

Weisz, P. B., and R. D. Goodwin, "Combustion of Carbonaceous Deposits within Porous Catalyst Particles: II. Intrinsic Burning Rate," *J. of Cat.*, **6**, 227 (1966).

Manuscript received May 16, 1988 and revision received Oct. 25, 1988.